

Pronounced summer warming in northwest Greenland during the Holocene and Last Interglacial

Jamie M. McFarlin^{a,1}, Yarrow Axford^a, Magdalena R. Osburn^a, Meredith A. Kelly^b, Erich C. Osterberg^b, and Lauren B. Farnsworth^b

^aDepartment of Earth and Planetary Sciences, Northwestern University, Evanston, IL 60208; and ^bDepartment of Earth Sciences, Dartmouth College, Hanover, NH 03755

Edited by Donald E. Canfield, Institute of Biology and Nordic Center for Earth Evolution, University of Southern Denmark, Odense M., Denmark, and approved April 27, 2018 (received for review November 22, 2017)

Projections of future rates of mass loss from the Greenland Ice Sheet are highly uncertain because its sensitivity to warming is unclear. Geologic reconstructions of Quaternary interglacials can illustrate how the ice sheet responded during past warm periods, providing insights into ice sheet behavior and important tests for data-model comparisons. However, paleoclimate records from Greenland are limited: Early Holocene peak warmth has been quantified at only a few sites, and terrestrial sedimentary records of prior interglacials are exceptionally rare due to glacial erosion during the last glacial period. Here, we discuss findings from a lacustrine archive that records both the Holocene and the Last Interglacial (LIG) from Greenland, allowing for direct comparison between two interglacials. Sedimentary chironomid assemblages indicate peak July temperatures 4.0 to 7.0 °C warmer than modern during the Early Holocene maximum in summer insolation. *Chaoborus* and chironomids in LIG sediments indicate July temperatures at least 5.5 to 8.5 °C warmer than modern. These estimates indicate pronounced warming in northwest Greenland during both interglacials. This helps explain dramatic ice sheet thinning at Camp Century in northwest Greenland during the Early Holocene and, for the LIG, aligns with controversial estimates of Eemian warming from ice core data retrieved in northern Greenland. Converging geologic evidence for strong LIG warming is challenging to reconcile with inferred Greenland Ice Sheet extent during the LIG, and the two appear incompatible in many models of ice sheet evolution. An increase in LIG snowfall could help resolve this problem, pointing to the need for hydroclimate reconstructions from the region.

Greenland | Holocene thermal maximum | Last Interglacial | Eemian | paleotemperature

Mean global surface temperature is projected to warm 1 to 4 °C by 2100, with amplification of surface temperatures in the Arctic two to four times that of the global mean (1, 2). In response, mass loss from the Greenland Ice Sheet (GrIS) is expected to increase, contributing up to ~0.2 m of global sea level rise by the end of this century (1). Estimates of sea level rise come largely from computational models. These models are tested with paleoclimate data-model comparisons, which depend upon reliable constraints on past climatic conditions. The insolation-driven warming of the Arctic in the Early Holocene (~11 to 8 ka) and the Last Interglacial Period (LIG; 129 to 116 ka) are key targets for data-model comparisons, providing important checks of the models used to project long-term warming and future ice sheet evolution (3). Notably, many model studies for these periods find that simulations invoking temperatures comparable with those implied by the few existing paleotemperature reconstructions from Greenland drive GrIS behavior that conflicts with inferred ice sheet extent (4–7). This highlights a need for additional paleoclimate records from Greenland that better resolve regional and seasonal conditions to provide stronger tests of climate and ice sheet models.

In Greenland, there are few quantitative air temperature reconstructions near the ice sheet margin for the Early Holocene and the LIG (Table 1; including records from nearby Baffin and

Ellesmere Islands). A lack of constraint on these conditions is a significant limitation in understanding past ice sheet behavior because summer temperatures along the ice sheet margins drive surface melt and thus exert a major control on mass balance of the dominantly land-based interglacial ice sheet (6, 8). Lakes on Greenland's ice-free margin provide opportunities to reconstruct paleoclimate via sedimentary climate proxies. While there are several Holocene climate reconstructions from Greenland lake sediments for the Middle to Late Holocene (9), to date, only one published lacustrine archive quantifying summer air temperature extends well into the Early Holocene (10) to overlap with maximum summer insolation and peak overall regional Holocene warmth inferred from ice cores (11, 12). The conventional picture of Greenland's climate during the Holocene Thermal Maximum (HTM) is of ~3 °C of roughly homogenous warming (12), and this typifies the maximum forcing applied (+2 to 4 °C vs. modern) across Greenland in simulations of Holocene ice sheet evolution (4, 5). However, a recent reinterpretation of ice $\delta^{18}\text{O}$ data from the Agassiz Ice Cap, the original results of which were influential in shaping perceptions of HTM climate over Greenland, revises peak Holocene precipitation-weighted temperatures at Agassiz upwards from the original reconstruction by ~3 °C (11). New evidence corroborating this surprising result would indicate large spatial variations in the magnitude of HTM warmth, including along the margins of the GrIS. As proposed by ref. 11, warmer regional

Significance

Reconstructions of climate over Greenland during past warm periods provide crucial insights into the likely response of the Greenland Ice Sheet to future warming. However, limited preservation of interglacial archives due to extensive glacial scouring has hindered paleoclimate reconstructions along Greenland's margins. Here, we report a Greenland lake sediment record that preserves both the present and previous interglacial periods. This record, combined with prior studies, demonstrates exceptionally strong warming over the northern Greenland Ice Sheet. Pronounced summer warming in this region helps explain ice sheet changes in the Early Holocene, while highlighting seemingly incongruous evidence for ice sheet extent and temperatures during the Last Interglacial. These findings may portend large future warming in this high-latitude region.

Author contributions: J.M.M., Y.A., and M.R.O. designed research; J.M.M., Y.A., M.A.K., E.C.O., and L.B.F. performed research; J.M.M., Y.A., M.A.K., and L.B.F. analyzed data; and J.M.M., Y.A., M.R.O., M.A.K., E.C.O., and L.B.F. wrote the paper.

The authors declare no conflict of interest.

This article is a PNAS Direct Submission.

Published under the PNAS license.

Data deposition: Enumerated assemblages, temperature reconstructions, and radiocarbon results are publicly available online at the National Oceanic and Atmospheric Administration Paleoclimate Database (<https://www.ncdc.noaa.gov/paleo/study/23990>).

¹To whom correspondence should be addressed. Email: jamie@earth.northwestern.edu.

This article contains supporting information online at www.pnas.org/lookup/suppl/doi:10.1073/pnas.1720420115/-DCSupplemental.

Table 1. Greenland/Baffin Bay region continental air temperature estimates

Site	Map	Proxy	Baseline	Season	Anomaly, °C	Source
Early Holocene						
Wax Lips Lake	WLL	Midges	AD 1952 to 2014	July	+5.5 ± 1.7	This study
Agassiz Ice Cap	A	Melt	AD 1750	Summer	+5, min of	(11)
		Ice δ ¹⁸ O	AD 1750	P-W	+6.1 ± 2.2	(11)
Last Chance Lake	1	Midges	Last millennium	July	+3 to 4 ± 1.5	(10)
Renland Ice Cap	R	Ice δ ¹⁸ O	AD 2000	P-W	+2 to 3	(12)
Lake CF8	2	Midges	AD 1961 to 1990	July	+4 to 5 ± 2.2	(31)
Lake CF3	3	Midges	AD 1951 to 1980	July	+4 to 6 ± 2.2	(59)
Last Interglacial						
Wax Lips Lake	WLL	Midges	AD 1952 to 2014	July	+7 ± 1.7	This study
Thule	T	Insects, plants	AD 1990s	Summer	+4	(13)
NEEM ice cores	Nm	Ice δ ¹⁸ O	Last millennium	P-W	+8 ± 4	(15)
		Air δ ¹⁵ N	Preindustrial	MAAT	+7 to 11	(25)
Jamesonland	J	Insects, plants	AD 1990s	Summer	+5	(14)
GISP2 ice cores	G	Ice δ ¹⁸ O	Last millennium	P-W	+4 to 8	(26)
Lake CF8	2	Midges	AD 1961 to 1990	July	+4 to 5 ± 2.2	(31)
Fog Lake	4	Pollen	AD 1971 to 2000	July	+4 to 5 ± 1.2	(60)
		Midges	AD 1971 to 2000	July	+3 to 4 ± 1.5	(35)
Brother of Fog Lake	5	Pollen	AD 1971 to 2000	July	+3 to 4 ± 1.2	(60)
		Midges	AD 1971 to 2000	July	+8 to 9 ± 1.5	(35)
Amorak Lake	6	Pollen	AD 1971 to 2000	July	+4 to 5 ± 1.2	(60)

Estimates derived from individual published sites. (Early Holocene) Average maximum air temperature anomaly for the Early Holocene from 11 to 8 ka or any recorded portion of that period. Archives that begin after 8 ka or are not securely dated to within this time are excluded. (Last Interglacial) Maximum air temperatures recorded in archives of the Last Interglacial. Note that estimates vary in timing within the LIG, in most cases, precise timing within the LIG is unknown, and, for most archives, it is uncertain if maximum local LIG temperatures are recorded. MAAT, mean annual air temperature; P-W, precipitation-weighted annual air temperature.

temperatures during the HTM could help explain otherwise puzzling ice sheet thinning at Camp Century in northwest Greenland (11, 12). Updated estimates of stronger warming over the northern GrIS, extrapolated from Agassiz, increased the GrIS modeled contribution to sea level rise during the last deglaciation by 1.4 m sea-level equivalent (11). These findings demonstrate that uncertainties in the magnitude of HTM warming significantly influence the simulations of ice sheet evolution for this period and underscore how sensitive the GrIS is to temperature.

Lake sediments were extensively eroded by expanded ice sheets during the last glacial period, so most LIG records from Greenland come from the GrIS itself and do not constrain the ice-marginal summer temperatures important to surface melt. There are two locations along Greenland's margin for which estimates of summer air temperature anomalies during some part of the LIG are available (Table 1; +4 to 5 °C vs. present) (13, 14). Furthermore, only the North Greenland Eemian Ice Drilling (NEEM) record definitively captures maximum LIG warmth. The peak precipitation-weighted temperature anomaly from ice δ¹⁸O reconstructed at NEEM for the LIG is +8 ± 4 °C relative to the last millennium (15). This strong inferred LIG warming has generally been perceived as a controversial outlier because syntheses of terrestrial climate reconstructions have reported average LIG warming across the Arctic and Greenland of ≤5 °C (16, 17), and most climate models simulate a temperature anomaly in north Greenland that is ≤5 °C (18–20). Ice δ¹⁸O-temperature relationships vary geographically and change through time (21) and are impacted by changes in elevation and ice sheet topography (22, 23). In modern ice at the NEEM site, an ice δ¹⁸O-temperature relationship of 1.1‰ °C⁻¹ was observed during recent warming (24); temperature anomalies for the LIG in the NEEM ice cores were calculated using a relationship from central Greenland of 0.5‰ °C⁻¹ (12, 15), perhaps resulting in an overestimation of LIG temperature at NEEM (21, 22). However, a subsequent LIG temperature reconstruction based on nitrogen isotopes (δ¹⁵N) measured in trapped air in NEEM ice cores, which estimates warming of 7 to 11 °C vs. preindustrial, supports the estimate from ice δ¹⁸O (25). A recent reanalysis of LIG ice at the Greenland Ice Sheet Project 2 (GISP2) site shows

4 to 8 °C of warming vs. the last millennium, further supporting warmer conditions during the LIG than previously inferred (26).

In contrast to ice core evidence for a LIG peak warming anomaly of 4 to 12 °C over the GrIS, geologic evidence indicates that GrIS area and thickness were only somewhat reduced relative to today. Total air content in NEEM and GISP2 ice suggests that LIG elevation of the GrIS at both localities was within several hundred meters of modern (15, 26). LIG-aged ice has been identified from deep core sites across Greenland [NEEM, North Greenland Ice Core Project (NGRIP), GRIP, GISP2, Dye 3, and Camp Century] (Fig. 1B) (27, 28). Along with sedimentologic evidence from the Eirik Drift for some enduring southern ice throughout the LIG (29), the ice core evidence indicates that much of the GrIS persisted through the LIG despite possible large losses of ice from some regions (27). This geologic picture of ice loss contributes to converging model estimates that the GrIS supplied 1 to 3 m of the 6 to 9 m of observed LIG sea-level rise and implies high sensitivity of the West Antarctic ice sheet to LIG warming (30). However, a major limitation to this conclusion is that LIG temperature estimates from Greenland are sparse and highly uncertain and therefore have been open to a wide range of interpretations. This is particularly the case for summer temperatures around ice margins and the seasonality of precipitation-weighted warming estimated from δ¹⁸O. For ice sheet models to sustain the requisite volume of ice on Greenland during the LIG, they must be forced by temperature anomalies <5 °C or even <2 °C, much cooler than temperatures inferred at NEEM and recently at GISP2 (6, 18, 26). Thus, the ice sheet models call the geologic data for temperature and GrIS extent into question, and vice versa. Resolving these issues for both the Holocene and the LIG requires more confident reconstructions across Greenland of air temperatures, precipitation amounts, and ice extent. Here, we report estimates of Holocene and LIG July air temperatures near the ice sheet margin in northwest Greenland, derived from the discovery of Holocene and LIG lake sediments preserved in situ in the extant lake that we informally designate Wax Lips Lake (WLL) (76.85°N, 66.96°W).

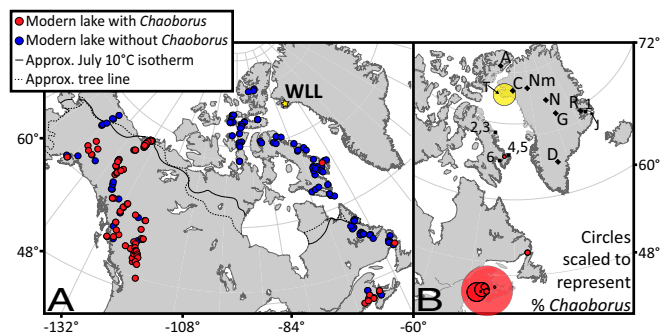


Fig. 1. (A) Location of WLL (yellow star) relative to modern July 10 °C isotherm (solid black line) and boreal tree line (dashed black line) (58). Lakes in two North American midge training sets (35, 41) with (red circles) and without (blue circles) *Chaoborus* in modern sediments. (B) Percentages of *Chaoborus* in modern sediments (red circles) vs. WLL LIG assemblages (yellow circle). Circles are scaled to represent percent of midge assemblage in each lake, with northernmost red circle <1%, largest red circle 13.5%, and yellow circle 6% *Chaoborus*. Locations of ice core archives (black diamonds) and lacustrine archives (black squares) are discussed in the text. A, Agassiz; C, Camp Century; D, Dye 3; G, GISP2; J, Jamesonland; N, NGRIP; Nm, NEEM; R, Renland; T, Thule; 1, Last Chance Lake; 2, Lake CF8; 3, Lake CF3; 4, Fog Lake; 5, Brother of Fog Lake; 6, Amarak Lake.

Results

WLL is a small (9 m deep, <1 km²) nonglacial lake situated 517 m above sea level in the highlands of northwest Greenland, 60 km east of Thule Air Base and 400 km west of the NEEM site (77.45°N, 51.06°W) (Fig. 1). WLL is 2 km from the current margin of the GrIS but topographically isolated from meltwater drainage. Several replicate sediment cores were obtained from WLL in 2012 and 2014 (Fig. 2). All are predominately composed of gyttja with abundant bryophyte material. Horizontal laminae are visible in X-radiographs throughout most of the record, including the basal sediments, illustrating intact stratigraphy (SI Appendix, Fig. S1). A major stratigraphic boundary is correlative across cores, manifesting as a color change from darker basal sediments to lighter brown gyttja above, and a corresponding step decrease in both magnetic susceptibility and density. Aquatic mosses preserved in the gyttja below this boundary yield accelerator mass spectrometry (AMS) ¹⁴C ages that predate the last glacial maximum (LGM) (four out of five are nonfinite) (SI Appendix, Table S1), whereas aquatic mosses above this boundary yield exclusively Holocene ¹⁴C ages and record lacustrine deposition throughout the Holocene. Given age uncertainties that result from multiple ¹⁴C age reversals within the Holocene sediments, we interpret the Holocene biostratigraphy at coarse temporal resolution. Living aquatic moss collected from WLL yielded a postbomb ¹⁴C age. The occurrence of nonfinite ¹⁴C ages immediately underlying Holocene ages indicates that the major stratigraphic boundary in the cores is an unconformity separating intact pre-LGM from Holocene sediments.

Similar in situ pre-LGM lake sediments have been documented in other Arctic regions with relict landscapes formerly overridden by cold-based (i.e., frozen-bedded and thus minimally erosive) ice (31, 32). Features on the landscape surrounding WLL are analogous to landscapes around lakes on Baffin Island that preserve LIG sediments despite having been overridden by a frozen-bedded portion of the Laurentide Ice Sheet (32), supporting a similar history at WLL. The GrIS expanded over WLL to reach its documented extent on the continental shelf during the LGM (33). Despite this, and like glaciated relict landscapes on Baffin Island, WLL is surrounded by a weathered highland landscape of tors and angular boulder fields, patterned ground, and minimal fine-grained sediments. Bedrock and glacially transported boulders on these highlands contain cosmogenic nuclide inheritance from prior periods of exposure (SI Appendix, Fig. S2) (34), providing local evidence for minimally erosive ice

cover during the LGM. The compacted nature of the pre-LGM sediments in WLL, reflected in higher magnetic susceptibility and density, is consistent with dewatering during compression by overriding nonerosive ice. Combined, the geomorphic and stratigraphic evidence indicates that cold-based ice advanced over WLL during the LGM and compacted and preserved pre-LGM lake sediments. The unconformity between pre-LGM and Holocene sediments in WLL represents a hiatus in deposition during glacial conditions and could also reflect some erosion of pre-LGM sediments that nonetheless left the underlying sedimentary structure intact.

We estimate mean July air temperatures based upon subfossil midge (Diptera: Chironomidae and Chaoboridae) assemblages, employing the climatically and biogeographically relevant training set of Francis et al. (35), which compiles calibration data from 68 northeast North American lakes spanning from the Canadian Arctic islands to Maine and a July air temperature range from 6 to 18 °C (35). The Francis et al. (35) dataset incorporates both Chironomidae and Chaoboridae, the latter of which is not enumerated in many other training sets. This training set has been used in east and west Greenland (10, 36) and in a comparable climate on Baffin Island ~700 km from WLL (31, 35). No midge-temperature calibration dataset is available from mid to high arctic Greenland. Squared-chord distances (SCDs) quantifying dissimilarity between subfossil assemblages and the training set demonstrate that almost all WLL samples have a very close modern analog (defined as SCD lower than—i.e., more similar than—the fifth percentile of SCDs in the training set), with just a few Late Holocene assemblages above this threshold (37, 38) (SI Appendix, Fig. S3).

Holocene Temperatures. Midge assemblages during the Early Holocene were characterized by the relatively thermophilous Tanypodinae and *Psectrocladius* and the absence of cold stenotherms that are abundant in the Late Holocene sediments of WLL and common in lakes in the high Arctic today (10, 35, 39). We estimate that July air temperatures were up to 4.0 to 7.0 °C warmer than modern (reference period AD 1952 to 2014) during the warmest millennia of the Holocene at WLL 10 to 8 ka (Fig. 3). We consider this an upper bound on warming because adjusting for postglacial isostatic rebound would reduce this estimate, although likely by a fraction of a degree (4). A 7,700-y record of lake water δ¹⁸O in Secret Lake (SL), 35 km southwest of WLL (40), is too young to record peak temperatures of the Early Holocene but indicates summer-biased warming of 2.5 to 4.0 ± ~2 °C vs. modern from 7.7 to 6.5 ka, providing a validation (agreement within model errors) of our estimates for this time and an independent loose lower bound on Holocene warmth in the region.

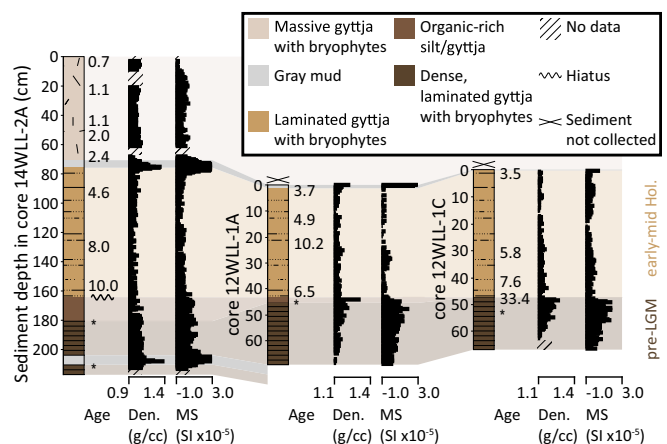


Fig. 2. Stratigraphy of three WLL cores, with calibrated ¹⁴C ages (cal ky BP), density (Den.), and magnetic susceptibility (MS). *, locations of nonfinite ¹⁴C samples.

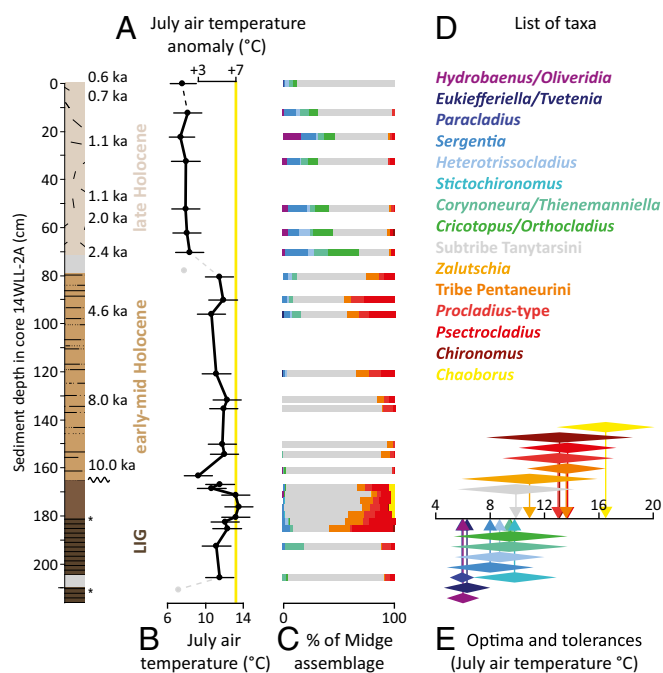


Fig. 3. Midge-inferred July air temperature at WLL as (A) anomalies relative to modern and (B) absolute temperatures. Yellow line marks anomaly of +7.0 °C. Gray points indicate samples from discrete glaciolacustrine units where midge assemblages may not accurately reflect air temperatures (*SI Appendix*). Error bars are model root mean square error of prediction ± 1.7 °C. (C) Percent of each midge type in subfossil assemblage, with colors corresponding to taxon names in D and modern optima and tolerances of taxa in the Francis et al. (35) training set, as shown in E. The apex of each diamond in E indicates optimum while length of diamond indicates tolerance.

Evidence for cooling in the late Holocene at WLL—a decline in warm-dwelling taxa and an increase in cold-dwelling taxa—mirrors isotope-based temperature estimates from SL (40). The coldest stenotherms, *Hydrobaenus/Oliveridia* (Fig. 3C and *SI Appendix*, Fig. S4), are most abundant at WLL during the coldest period at SL, suggesting that these nearby lakes cooled in unison through the late Holocene. However, we note that WLL temperatures inferred from midges plateau throughout the coldest part of the Holocene 2.5 to 0.5 ka (40). This reflects a known limitation of our method: The training set includes few calibration sites colder than our study site, limiting its utility for reconstructing very cold past climates (10, 31, 35, 36). This does not affect temperature estimates for periods warmer-than-present at WLL because the reconstructed warmer temperatures are well within the range of the calibration data (6 to 18 °C), and these downcore assemblages have close modern analogs in the training set.

Pre-LGM Temperatures and Assignment of the Pre-LGM Unit to the Last Interglacial. The pre-LGM sediments at WLL record peak July air temperatures 5.5 to 8.5 °C warmer than modern, with this warmth supported by the presence of up to 6% of the currently extralimital “phantom midge” *Chaoborus* (Fig. 3C and *SI Appendix*, Fig. S5). In North American training sets, *Chaoborus* are mostly found at latitudes south of the 10 °C July isotherm (35, 41) (Fig. 1A), and they are abundant (>1.5%) only at the lowest latitudes of our calibration dataset (35) (e.g., in Labrador) (Fig. 1B). To our knowledge, neither extant nor subfossil *Chaoborus* have previously been reported from Greenland (42, 43), and *Chaoborus* are absent from the Holocene sediments of WLL. Other relatively warm-dwelling taxa, including *Chironomus* and Tanyptodinae, achieve peak abundance in the pre-LGM sediments.

Although there are no absolute dates for the pre-LGM unit of WLL, we confidently assign it to the LIG because of the following. (i) Nonfinite ^{14}C ages indicate that this unit is >45,000 y old. (ii) Thermophilous midge assemblages constrain it to a period of sustained full interglacial warmth, exceeding the maximum temperatures of the Holocene. The LIG/Eemian is the most recent known period of sustained temperatures warmer than the Early Holocene in the Arctic. (iii) Glacial geologic evidence including ^{10}Be dates support cold-based conditions at the site during the most recent glacial period. Thus, the geologic setting permitted preservation of LIG sediments whereas the probability of preserving sediments from an even older warm period, but not from the LIG, is very low.

The long glacial period between the LIG and Holocene is represented by a hiatus in deposition. Although *Hydrobaenus/Oliveridia* at the top of the pre-LGM unit suggests declining temperature after the LIG maximum, we cannot rule out some erosion of LIG sediments. Therefore, we cannot be certain that we capture the entire LIG, and the maximum temperature anomaly reconstructed at WLL should be viewed as a minimum constraint on peak LIG warmth.

Discussion

At WLL, peak July air temperatures of the Early Holocene 10 to 8 ka are estimated at up to 4.0 to 7.0 °C warmer than modern and overlap in time with the Northern Hemisphere maximum in summer insolation (8). The onset of sediment accumulation in WLL ~10 ka indicates a rapid deglaciation of the nearby GrIS margin, having receded to at least near its present-day position by that time. Reconstructed LIG temperatures are at least 5.5 to 8.5 °C warmer than modern at WLL. Unlike the HTM, LIG warming was associated with the migration of the presently extralimital taxon *Chaoborus* to WLL (43), suggestive of a significant northward migration of boreal climate conditions during the LIG (44). This inference is also supported by low and subarctic terrestrial and marine fauna preserved in fluvial and raised shallow marine sediments near Thule and Jamesonland in east Greenland (13, 14, 45, 46). Results at WLL are consistent with prior studies showing that peak Arctic warmth during the LIG exceeded that of the HTM, consistent with the larger insolation anomaly and earlier penultimate deglaciation in the LIG (17). The magnitude of warming during both periods over northwest Greenland suggests that strong positive feedbacks may enhance warming in this region, which could portend stronger-than-predicted warming there in the future. Importantly, WLL temperature estimates reflect summer conditions near the GrIS margin: i.e., the season and setting that control ice sheet surface melt (6, 8).

The amplitude of our HTM summer temperature anomaly agrees with the minimum bound on Early Holocene summer warming of 3 to 4 °C vs. modern inferred from melt on Agassiz Ice Cap ~500 km to the northwest of WLL (11). WLL estimates of summer HTM climate for northwest Greenland are ~2 °C warmer than both the previous estimates of precipitation-weighted (annually integrated) warming over Greenland (ref. 12; reinterpreted in ref. 11) and recent simulations of Early Holocene summer temperatures in the Thule/Camp Century region (8). Evidence for strong warming in the Early Holocene contradicts some Holocene climate models that suggest delayed and attenuated HTM warming here due to effects from the waning Laurentide Ice Sheet (47).

In simulations of the Holocene evolution of the GrIS, imposed HTM warming is typically extrapolated from central Greenland and assumed to be relatively homogenous across broad regions of the ice sheet (4, 5). The use of more resolved temperature forcings is limited by a lack of paleotemperature estimates for the HTM from Greenland’s margin. Thus, extrapolated and/or scaled temperature forcings are currently a large source of unavoidable uncertainty in such simulations (4, 5). Many models fail to capture the 0.5 to 1 km of thinning registered at Camp Century in the Early Holocene (4, 48) without applying a larger

temperature anomaly at Camp Century (11). WLL is situated ~150 km from Camp Century and provides an independent estimate of local summer temperature. The +4.0 to 7.0 °C temperature anomaly from 10 to 8 ka at WLL matches well with a modeled temperature time series for Camp Century based on the revised Agassiz reconstruction (11). Together, these studies help explain dramatic thinning observed at Camp Century and quantify the regional summer air temperatures associated with Holocene elevation change.

The reconstructed strong LIG warming at WLL of at least 5.5 to 8.5 °C vs. modern is consistent with the controversial estimate of 8 ± 4 °C precipitation-weighted warming vs. the last millennium at NEEM (15). This estimate from WLL is warmer than prior estimates of +4 to 5 °C vs. modern from biotic remains preserved in discontinuous terrestrial deposits near the Thule Air Base (13). However, given likely incomplete preservation, these prior results provide a minimum bound on local LIG warmth. Agreement between the anomalies at WLL and NEEM suggests that ice $\delta^{18}\text{O}$ precipitation-weighted temperature was strongly summer-biased at NEEM during the LIG, or else there was also significant isotopic enrichment of nonsummer precipitation, possibly from a longer period of sea ice-free conditions in Baffin Bay (24, 49), and/or similarly large average annual warming due to changes in atmospheric circulation (50). Together, the WLL, Agassiz Ice Cap, and NEEM records provide evidence from multiple sites and proxies for strong HTM and LIG summer warming over northern Greenland and Ellesmere Island—Earth's largest land masses at such a northerly latitude. Only a subset of climate models of the HTM and LIG simulate the warmest continental temperature anomalies at these very highest Arctic latitudes (8, 19, 20). Paleoclimate data here and elsewhere (16, 17) support this subset of models.

For the LIG, evidence for intense summer warming over northern Greenland exacerbates the paradox embodied at NEEM (6) where data indicate both strong LIG warming and, in contrast, only a relatively modest reduction in ice sheet thickness (-130 ± 300 m relative to present) (15, 26). Ice sheet models thus far cannot simultaneously accommodate observations of large warming over the GrIS and geologic evidence for a widespread GrIS throughout the LIG (6, 26, 51). This paradox could be resolved if LIG summer warming was localized to the central ice sheet, or LIG warming was relatively weak in summer, limiting surface melt (6). However, WLL temperature estimates reflect pronounced summer warming at the margin of the GrIS and thus argue against both explanations. Nor is it likely that the northern GrIS is somehow inherently insensitive to warming: To the contrary, some models have suggested that the arid northern GrIS may be especially sensitive to warming (7, 52), and dramatic GrIS thinning at Camp Century during the HTM also challenges this notion (11). Furthermore, intense warming was not necessarily unique to the northernmost part of the ice sheet: GISP2 (Summit) does not definitively capture peak warmth during the Early LIG but now provides a minimum constraint on peak LIG anomalies of +4 to 8 °C over central Greenland (26). Collectively and based upon multiple independent proxies, the WLL, NEEM, and GISP2 records point to larger LIG warming across Greenland than the +4 to 5 °C hitherto often estimated (16, 17).

Greater snow accumulation over north Greenland during the LIG might help resolve the LIG paradox in this region (53). There is some evidence for increased snowfall in west Greenland during the HTM (54) although it was apparently not enough to counteract ice sheet thinning at Camp Century (11). Current paleoclimate data poorly constrain LIG snowfall over Greenland, and models suggest relatively modest LIG increases in snowfall (52), but the hypothesis of greater accumulation during the LIG is supported by recent observations for a strong relationship between accumulation and temperature at the NEEM site (24) and evidence for greater accumulation during the LIG than the Holocene at Summit (26). Additional reconstructions of LIG precipitation, temperatures,

and ice sheet configuration are urgently needed to formulate stronger paleoclimate model-data comparisons and ultimately to further improve models of Greenland's climate and ice sheet behavior.

Conclusions

July air temperature estimates at WLL indicate pronounced warming during both the HTM and the LIG. The data presented here from a rare lake record of two interglacials agree with previous disparate reconstructions of exceptional warming over Ellesmere Island for the HTM and northern Greenland during the LIG, illustrating consistently strong regional warming during interglacials. Strong summer warming over northern Greenland, demonstrated by temperature anomalies at WLL of up to +4.0 to 7.0 °C for the HTM and at least +5.5 to 8.5 °C for the LIG, should be accommodated in future paleoclimate simulations and models of ice sheet evolution. In addition, if this large magnitude of HTM and LIG warming resulted from cryospheric or other feedbacks, such strong warming at WLL may portend even larger changes over this region than predicted in the coming century, as the Arctic warms to levels unprecedented since the LIG (1, 27).

Materials and Methods

For ^{10}Be dating, we sampled flat-lying upper surfaces of quartz-rich, stable perched boulders and bedrock and avoided surfaces that experienced past water cover as evidenced by traces of former lake levels. ^{10}Be samples were processed at Dartmouth College, and $^{10}\text{Be}/\beta\text{Be}$ was measured at the Center for Accelerator Mass Spectrometry at Lawrence Livermore National Laboratory, following standard procedures as described in the *SI Appendix*. Ages were calculated using the Cosmic Ray-Produced Nuclide Systematics-Earth online calculator (55) with the Baffin Bay/Arctic production rate (56). Ages are reported in the *SI Appendix*, Fig. S2 and Table S2.

Cores were collected from the depocenter of WLL using a modified-Bolivia percussion coring system in 2012 and a Nesje percussion coring system in 2014 (*SI Appendix*, Table S3). Some cores intentionally bypassed surface sediments to maximize recovery of older sediments. Measurements of magnetic susceptibility and gamma density followed standard procedures, as described in *SI Appendix*. ^{14}C AMS ages were obtained on aquatic plant macrofossils picked from intact laminations and analyzed at the Woods Hole Oceanographic Institution-National Ocean Sciences Accelerator Mass Spectrometry facility. Age calibration followed standard practices described in *SI Appendix*.

Preparation and classification of midge subfossils followed standard methods as described in *SI Appendix*. July air temperatures were modeled using the Francis et al. (35) training set (44 taxa; $r^2_{\text{boot}} = 0.88$; root mean SE of prediction = 1.7 °C) (35). We use bootstrapping but otherwise follow the protocol of Francis et al. (35) for the model parameters yielding best model performance: Assemblage data were square root-transformed, and temperature estimates were derived from a weighted-average model using inverse deshrinking and tolerance down-weighting. Modern (AD 1952 to 2014) mean July air temperature at the coastal Thule (Pituffik) weather station is 5.2 °C (57). We observed with air temperature loggers deployed at our field sites in 2012 to 2014 that July air temperature at WLL is 1 °C warmer than at Thule, and estimated modern July air temperature for the reference period (AD 1952 to 2014) at WLL as 6.2 °C. Modern analog technique (MAT) was used to calculate dissimilarity between WLL subfossil samples and the training set, as squared-chord distances on untransformed assemblage data (37, 38).

ACKNOWLEDGMENTS. We thank the people and government of Greenland for site access (sample export permit 028/2014). M. Bigl, G. Bromley, M. Jackson, G. E. Lasher, E. Roy, J. Thompson, L. Corbett, E. Lutz, and A. Taylor assisted with field work; and the Thule Air Base, Air Greenland, the United States Air Force, J. Hurley, K. Cospoer, and Polar Field Services provided logistical support. C. Carrio, G. Schellinger, and T. Stilson helped in the laboratory at Northwestern. LacCore, the Woods Hole Oceanographic Institution National Ocean Sciences Accelerator Mass Spectrometry facility, the Center for Accelerator Mass Spectrometry at Lawrence Livermore National Laboratory, and J. P. Brown and the Field Museum provided additional analytical support. Maps were created using The Generic Mapping Tools. J. Townsend, C. Kuzawa, and two anonymous reviewers provided thoughtful comments on the manuscript. This work was funded by the National Science Foundation (NSF) Division of Polar Programs (Awards 1108306 and 1107411), the NSF CAREER Program (Award 1454734), an NSF Graduate Research Fellowship, the Geological Society of America, and the Institute for Sustainability and Energy at Northwestern.

1. Collins M, et al. (2013) Long-term climate change: Projections, commitments and irreversibility. *Climate Change 2013: The Physical Science Basis. Contribution of Working Group I to the Fifth Assessment Report of the Intergovernmental Panel on Climate Change*, eds Stocker TF, et al. (Cambridge Univ Press, Cambridge, UK), pp 1029–1136.
2. Miller GH, et al. (2010) Arctic amplification: Can the past constrain the future? *Quat Sci Rev* 29:1779–1790.
3. Marcott SA, Shakun JD, Clark PU, Mix AC (2013) A reconstruction of regional and global temperature for the past 11,300 years. *Science* 339:1198–1201.
4. Lecavalier BS, et al. (2014) A model of Greenland ice sheet deglaciation constrained by observations of relative sea level and ice extent. *Quat Sci Rev* 102:54–84.
5. Simpson MJR, Milne GA, Huybrechts P, Long AJ (2009) Calibrating a glaciological model of the Greenland ice sheet from the Last Glacial Maximum to present-day using field observations of relative sea level and ice extent. *Quat Sci Rev* 28: 1631–1657.
6. Goelzer H, Huybrechts P, Loutre M-F, Fichefet T (2016) Last Interglacial climate and sea-level evolution from a coupled ice sheet-climate model. *Clim Past* 12:2195–2213.
7. Stone EJ, Lunt DJ, Annan JD, Hargreaves JC (2013) Quantification of the Greenland ice sheet contribution to Last Interglacial sea level rise. *Clim Past* 9:621–639.
8. Buizert C, et al. (2018) Greenland-wide seasonal temperature reconstructions for the last deglaciation. *Geophys Res Lett* 45:1905–1914.
9. Briner JP, et al. (2016) Holocene climate change in Arctic Canada and Greenland. *Quat Sci Rev* 147:340–364.
10. Axford Y, et al. (2017) Timing and magnitude of early to middle Holocene warming in East Greenland inferred from chironomids. *Boreas* 46:678–687.
11. Lecavalier BS, et al. (2017) High Arctic Holocene temperature record from the Agassiz ice cap and Greenland ice sheet evolution. *Proc Natl Acad Sci USA* 114:5952–5957.
12. Vinther BM, et al. (2009) Holocene thinning of the Greenland ice sheet. *Nature* 461: 385–388.
13. Bennike O, Böcher J (1992) Early Weichselian interstadial land biotas at Thule, northwest Greenland. *Boreas* 21:111–118.
14. Bennike O, Böcher J (1994) Land biotas of the last interglacial/glacial cycle on Jameson Land, East Greenland. *Boreas* 23:479–487.
15. Dahl-Jensen D, et al.; NEEM community members (2013) Eemian interglacial reconstructed from a Greenland folded ice core. *Nature* 493:489–494.
16. Turney CSM, Jones RT (2010) Does the Agulhas Current amplify global temperatures during super-interglacials? *J Quat Sci* 25:839–843.
17. CAPE Last Interglacial project members (2006) Last Interglacial Arctic warmth confirms polar amplification of climate change. *Quat Sci Rev* 25:1383–1400.
18. Capron E, et al. (2014) Temporal and spatial structure of multi-millennial temperature changes at high latitudes during the Last interglacial. *Quat Sci Rev* 103:116–133.
19. Bakker P, et al. (2014) Temperature trends during the present and last interglacial periods—A multi-model-data comparison. *Quat Sci Rev* 99:224–243.
20. Lunt DJ, et al. (2013) A multi-model assessment of last interglacial temperatures. *Clim Past* 9:699–717.
21. Sime LC, et al. (2013) Warm climate isotopic simulations: What do we learn about interglacial signals in Greenland ice cores? *Quat Sci Rev* 67:59–80.
22. Sjolte J, Hoffmann G, Johnsen SJ (2014) Modelling the response of stable water isotopes in Greenland precipitation to orbital configurations of the previous interglacial. *Tellus B Chem Phys Meteorol* 66:1–16.
23. Merz N, Born A, Raible CC, Fischer H, Stocker TF (2014) Dependence of Eemian Greenland temperature reconstructions on the ice sheet topography. *Clim Past* 10: 1221–1238.
24. Masson-Delmotte V, et al. (2015) Recent changes in north-west Greenland climate documented by NEEM shallow ice core data and simulations, and implications for past-temperature reconstructions. *Cryosph* 9:1481–1504.
25. Landais A, et al. (2016) How warm was Greenland during the last interglacial period? *Clim Past* 12:1933–1948.
26. Yau AM, Bender ML, Robinson A, Brook EJ (2016) Reconstructing the last interglacial at Summit, Greenland: Insights from GISP2. *Proc Natl Acad Sci USA* 113:9710–9715.
27. Masson-Delmotte V, et al. (2013) Information from paleoclimate archives. *Climate Change 2013: The Physical Science Basis. Contribution of Working Group I to the Fifth Assessment Report of the Intergovernmental Panel on Climate Change*, eds Stocker TF, et al. (Cambridge Univ Press, Cambridge, UK), pp 383–464.
28. Andersen KK, et al.; North Greenland Ice Core Project members (2004) High-resolution record of Northern Hemisphere climate extending into the last interglacial period. *Nature* 431:147–151.
29. Colville EJ, et al. (2011) Sr-Nd-Pb isotope evidence for ice-sheet presence on southern Greenland during the Last Interglacial. *Science* 333:620–623.
30. Dutton A, et al. (2015) Sea-level rise due to polar ice-sheet mass loss during past warm periods. *Science* 349:aaa4019.
31. Axford Y, et al. (2011) Chironomids record terrestrial temperature changes throughout Arctic interglacials of the past 200,000 yr. *Bull Geol Soc Am* 123: 1275–1287.
32. Briner JP, Axford Y, Forman SL, Miller GH, Wolfe AP (2007) Multiple generations of interglacial lake sediment preserved beneath the Laurentide ice sheet. *Geology* 35: 887–890.
33. Funder S, Kjeldsen KK, Kjær KH, Cofaigh CÓ (2011) The Greenland ice sheet during the past 300,000 years: A review. *Dev Quat Sci* 15:699–713.
34. Farnsworth LB, et al. (2018) Holocene history of the Greenland Ice-Sheet margin in Northern Nunatassuaq, Northwest Greenland. *Arktos J Arct Geosci* 4:10.
35. Francis DR, Wolfe AP, Walker IR, Miller GH (2006) Interglacial and Holocene temperature reconstructions based on midge remains in sediments of two lakes from Baffin Island, Nunavut, Arctic Canada. *Palaeogeogr Palaeoclimatol Palaeoecol* 236: 107–124.
36. Axford Y, et al. (2013) Holocene temperature history at the western Greenland Ice Sheet margin reconstructed from lake sediments. *Quat Sci Rev* 59:87–100.
37. Overpeck JT, Webb T, III, Prentice IC (1985) Quantitative interpretation of fossil pollen spectra: Dissimilarity coefficients and the method of modern analogs. *Quat Res* 23: 87–108.
38. Simpson GL (2007) Analogue methods in palaeoecology: Using the analogue package. *J Stat Softw* 22:1–29.
39. Fortin M-C, et al. (2015) Chironomid-environment relations in northern North America. *J Paleolimnol* 54:223–237.
40. Lasher GE, et al. (2017) Holocene temperatures and isotopes of precipitation in northwest Greenland recorded in lacustrine organic materials. *Quat Sci Rev* 170: 45–55.
41. Barley EM, et al. (2006) A northwest North American training set: Distribution of freshwater midges in relation to air temperature and lake depth. *J Paleolimnol* 36: 295–314.
42. Borkent A (1993) A world catalogue of fossil and extant Corethrellidae and Chaoboridae (Diptera), with a listing of references to keys, bionomic information and descriptions of each known life stage. *Insect Syst Evol* 24:1–24.
43. Jensen DB, Christensen KD, eds (2003) The Biodiversity of Greenland—A Country Study (Pinngortiteriffik, Grønlands Naturinstitut, Nuuk, Greenland), Technical Report no. 55, p 165.
44. Taylor DJ, Ballinger MJ, Medeiros AS, Kotov AA (2015) Climate-associated tundra thaw pond formation and range expansion of boreal zooplankton predators. *Ecography* 39:43–53.
45. Kelly M, et al. (1999) Quaternary glacial and marine environmental history of northwest Greenland: A review and reappraisal. *Quat Sci Rev* 18:373–392.
46. Funder S (1990) Late Quaternary stratigraphy and glaciology in the Thule area, northwest Greenland. *Medd Gronl Geosci* 22:1–63.
47. Zhang Y, Renssen H, Seppä H (2016) Effects of melting ice sheets and orbital forcing on the early Holocene warming in the extratropical Northern Hemisphere. *Clim Past* 12:1119–1135.
48. Lecavalier BS, et al. (2013) Revised estimates of Greenland ice sheet thinning histories based on ice-core records. *Quat Sci Rev* 63:73–82.
49. Steen-Larsen HC, et al. (2011) Understanding the climatic signal in the water stable isotope records from the NEEM shallow firn/ice cores in northwest Greenland. *J Geophys Res Atmos* 116:1–20.
50. Cohen J, et al. (2014) Recent Arctic amplification and extreme mid-latitude weather. *Nat Geosci* 7:627–637.
51. Otto-Bliesner BL, Marshall SJ, Overpeck JT, Miller GH, Hu A (2006) Simulating Arctic climate warmth and icefield retreat in the last interglaciation. *Science* 311:1751–1753.
52. Born A, Nisancioglu KH (2012) Melting of Northern Greenland during the last interglaciation. *Cryosph* 6:1239–1250.
53. Helsen MM, van de Berg WJ, van de Wal RSW, van den Broeke MR, Oerlemans J (2013) Coupled regional climate-ice-sheet simulation shows limited Greenland ice loss during the Eemian. *Clim Past* 9:1773–1788.
54. Thomas EK, Briner JP, Ryan-Henry JJ, Huang Y (2016) A major increase in winter snowfall during the middle Holocene on western Greenland caused by reduced sea ice in Baffin Bay and the Labrador Sea. *Geophys Res Lett* 43:5302–5308.
55. Balco G, Stone JO, Lifton NA, Dunai TJ (2008) A complete and easily accessible means of calculating surface exposure ages or erosion rates from ¹⁰Be and ²⁶Al measurements. *Quat Geochronol* 3:174–195.
56. Young NE, et al. (2013) Age of the Fjord Stade moraines in the Disko Bugt region, western Greenland, and the 9.3 and 8.2 ka cooling events. *Quat Sci Rev* 60:76–90.
57. Wong GJ, et al. (2015) Coast-to-interior gradient in recent northwest Greenland precipitation trends (1952–2012). *Environ Res Lett* 10:114008.
58. D’Odonorico P, et al. (2013) Vegetation-microclimate feedbacks in woodland-grassland ecotones. *Glob Ecol Biogeogr* 22:364–379.
59. Briner JP, et al. (2006) A multi-proxy lacustrine record of Holocene climate change on northeastern Baffin Island, Arctic Canada. *Quat Res* 65:431–442.
60. Fréchet B, Wolfe AP, Miller GH, Richard PJH, de Vernal A (2006) Vegetation and climate of the last interglacial on Baffin Island, Arctic Canada. *Palaeogeogr Palaeoclimatol Palaeoecol* 236:91–106.